SUPPORTING INFORMATION

Fully waste recycling strategies for improving the accessibility of rice protein film

Chengxin He, Yu Hu, Yong Wang, Yang Liao, Hua Xiong, Cordelia Selomulya, Juwu Hu, Qiang Zhao*

Supporting figures

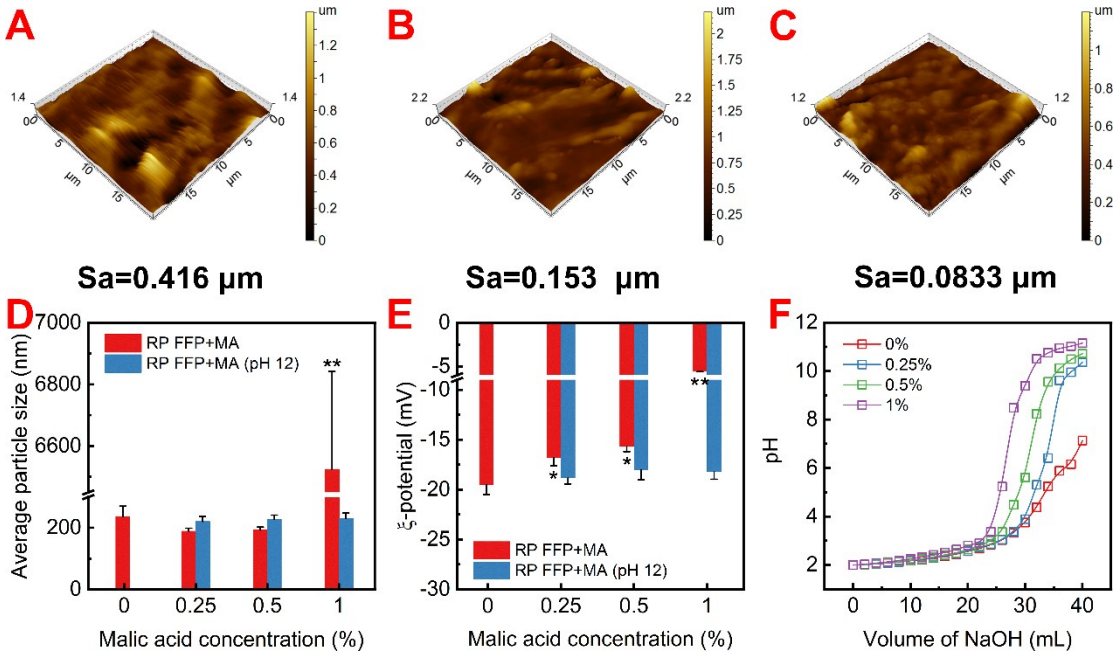

Fig. S1 Different concentrations (0% (A), 0.1% (B), 0.5% (C), 1%, unable to form self-stand film, w/v) of MA in RP FFP to prepare the film, and the surface roughness parameter SA measured by AFM; The average particle size (D) and ξ–potential (E) of RP FFP with different concentrations of MA (0%, 0.25%, 0.5%, and 1%, w/v) that adjusted to pH 12 or not; The typical titration curves of dispersion (pH 2) of RP which was co-heating with different concentrations of MA (0%, 0.25%, 0.5%, and 1%, w/v) titrated by 0.025 M NaOH. (*$p < 0.05$,**$p < 0.01$)

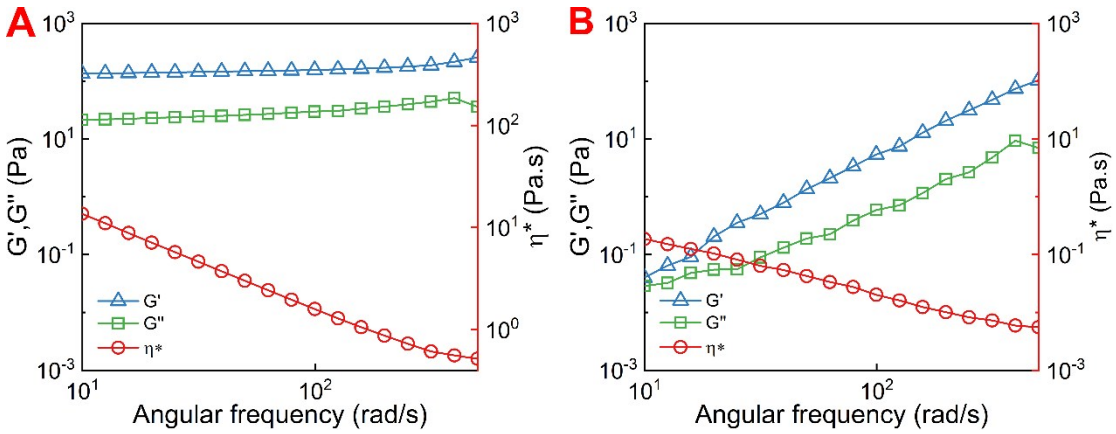

Fig. S2. The storage modulus (G'), loss modulus (G'') and the complex viscosity (η*) as a function of the angular frequency of PR-FFP (A) and RP-CPP FFP (B).

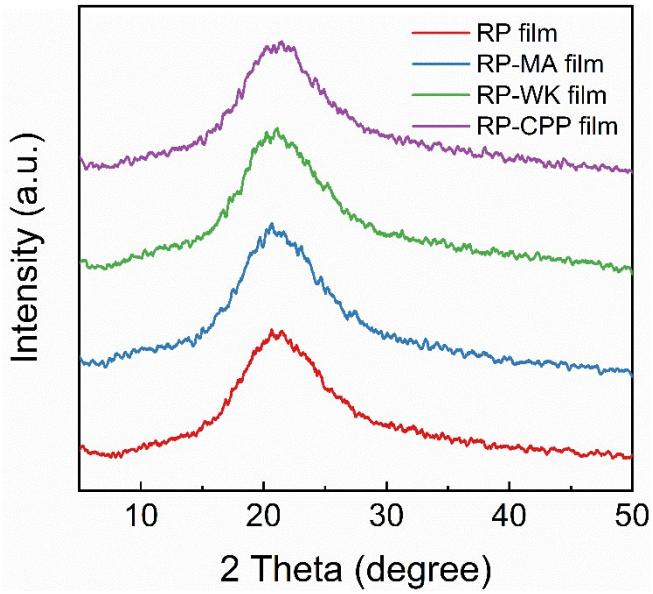

Fig. S3. The XRD intensity of PR film, RP-MA film,RP-WK film and RP-CPP film. from 5° to 50°.

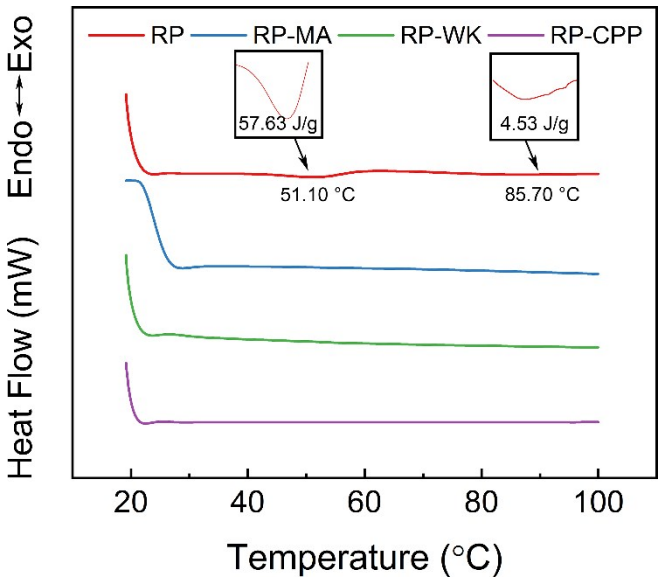

Fig. S4. DSC thermograms of RP, RP-MA FFP, RP-WK FFP, RP-CPP FFP from 20-100 °C.

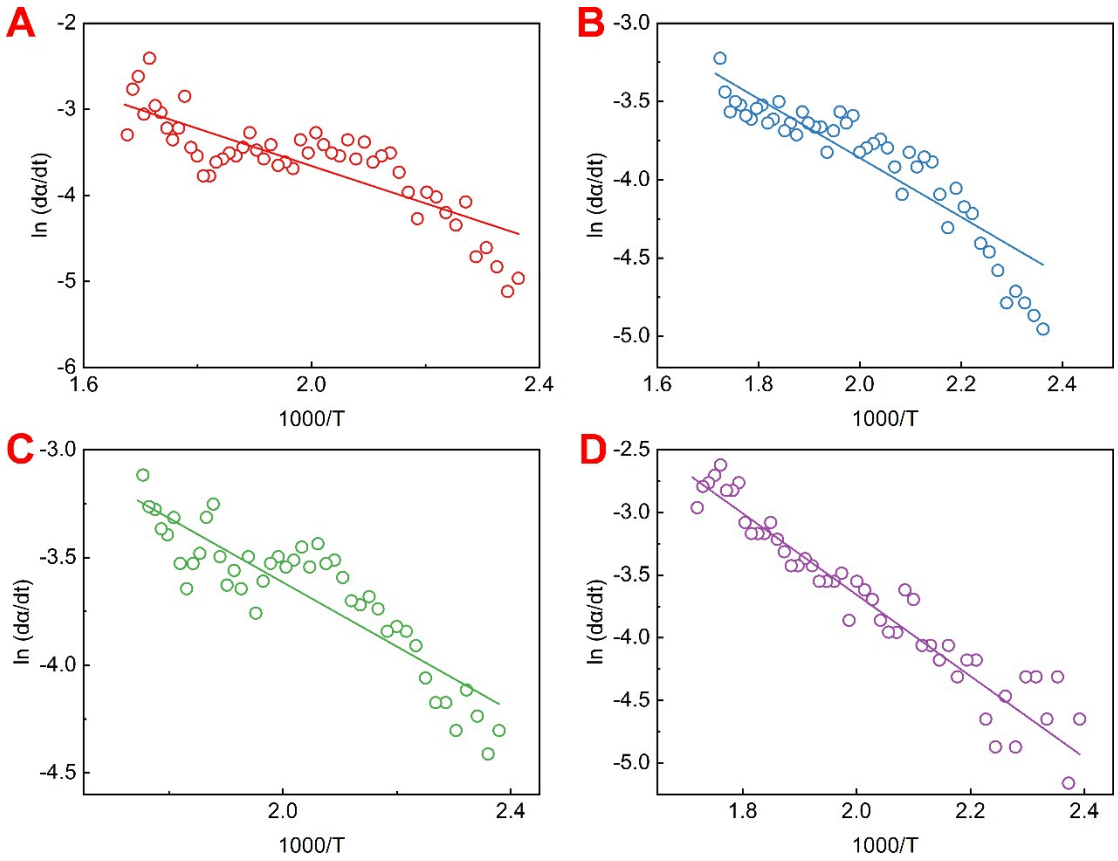

Fig. S5. A scatter plot of 1000/T and $\ln(\frac{d\alpha}{dt})$ was drawn (one dot was drow out every 20 points) with a slope equal to -E/R.

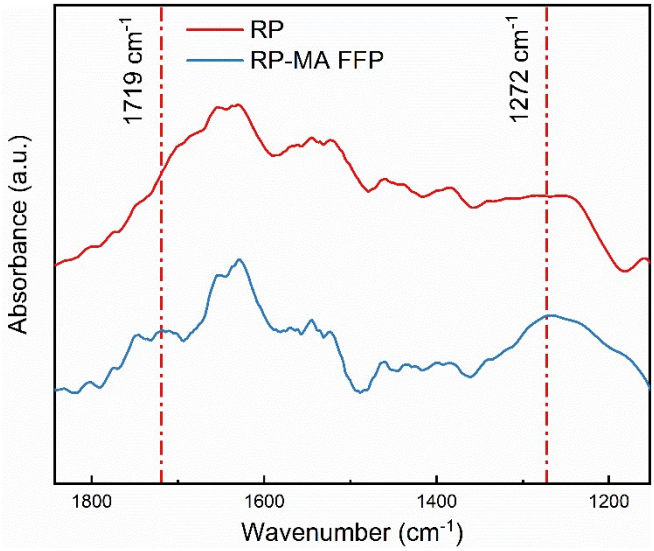

Fig. S6. FT-IR absorbance spectra of RP and RP-MA FFP about 1200~1800 cm^{-1}, and the dash dot indicates the designation of 1719 cm^{-1} and 1272 cm^{-1}.

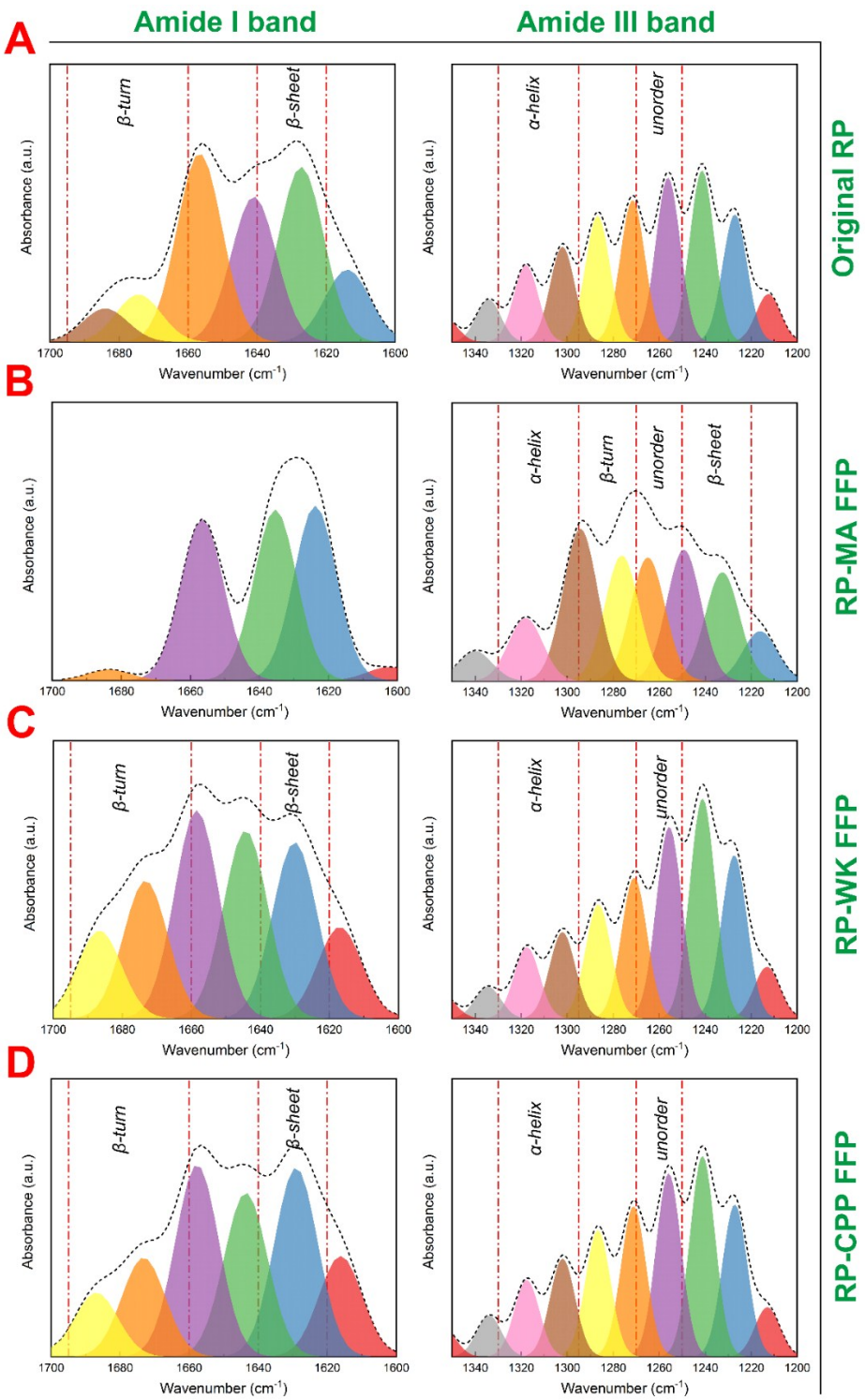

Fig. S7. Multi-peak Gaussian fitting of spectrum of the Original RP (A), RP-MA FFP (B), RP-WK FFP (C) and RP-CPP FFP (D) in amide I and amide III band: The short dash stands the fitting of the second derivative spectrum, and the dash dot indicates the designation of the secondary structure.

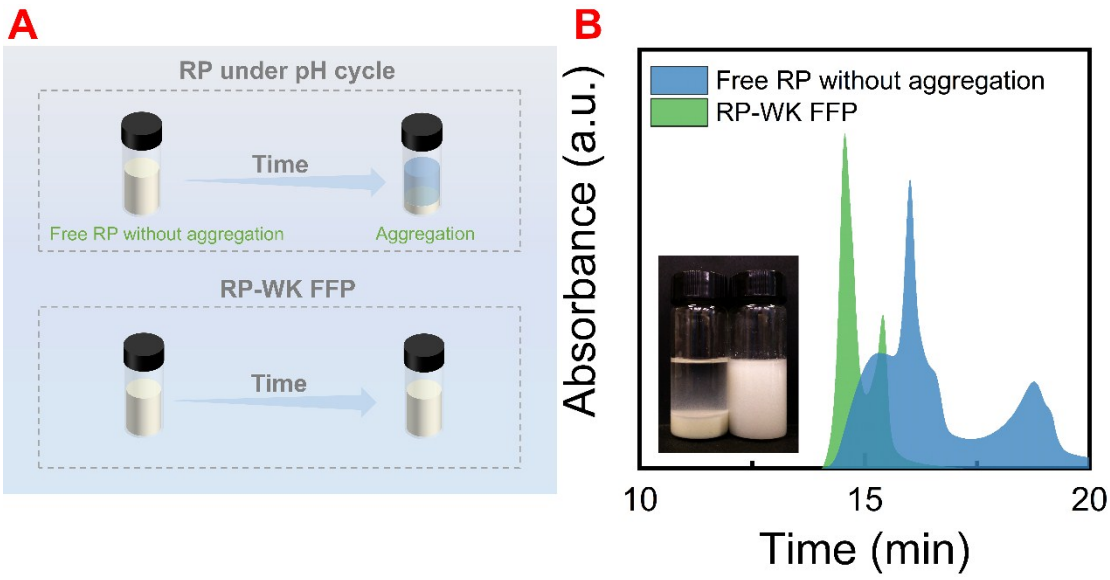

34

35 **Fig. S8.** (A) RP under pH cycle was prepared by the same steps as RP-WK FFP without the

36 addition of WK. After a period of time, RP under pH cycle will aggregate, while RP-WK

37 FFP not; (B) SEC-HPLC of free RP without aggregation and RP-WK FFP; The illustrations

38 are visual images of RP under pH cycle (left) and RP-WK FFP (right) after a period of time.

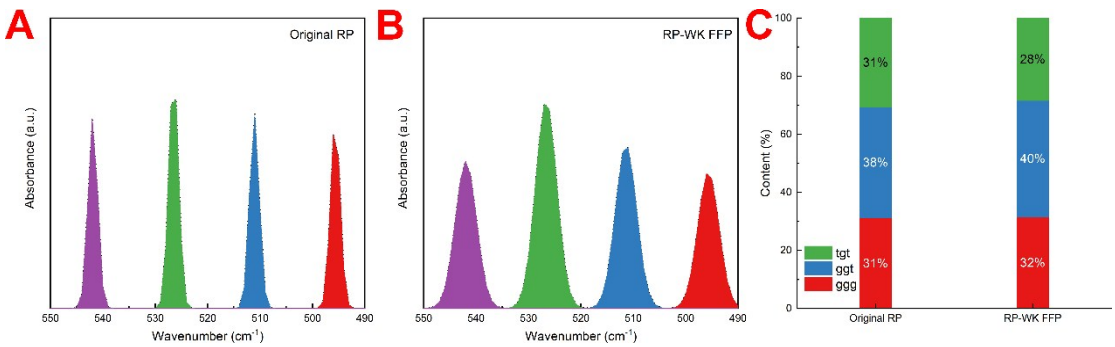

Fig. S9. Multi-peak Gaussian fitting of disulfide bonds in original RP (A) and RP-WK FFP (B) in 490–550 cm^{-1}, the short dash stands the fitting of the second derivative spectrum; The conformations content of C–S bond of original RP and RP-WK FFP (C).

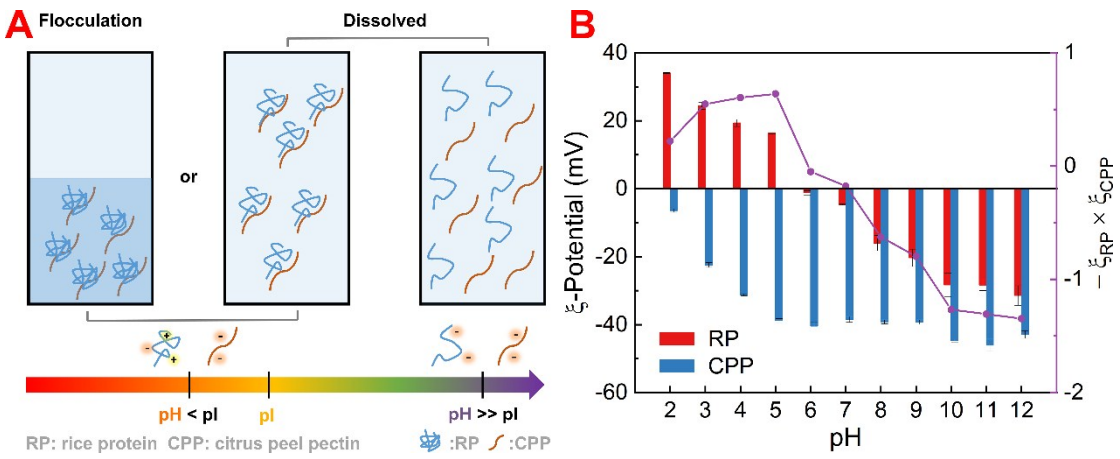

Fig. S10. Possible mechanisms of protein and polysaccharide interactions at different pH (A). The ξ- potential (B) of RP and CPP solution at different pH.

47

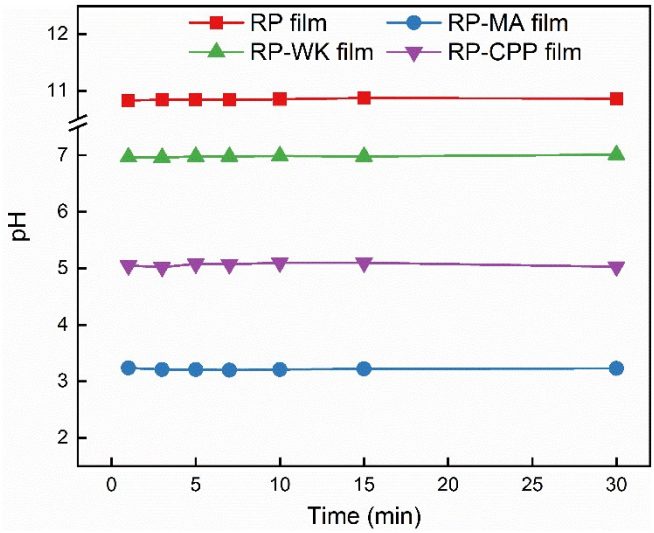

48 **Fig. S11.** The pH of protein film aqueous extract versus times.

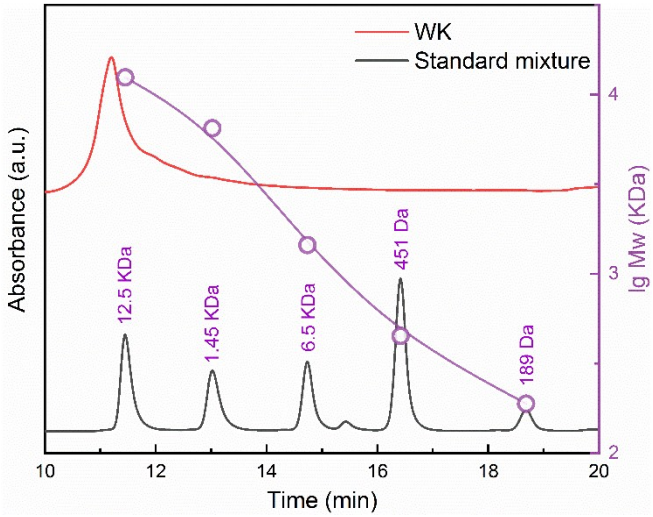

Fig. S12. SEC-HPLC of standard mixtures and regenerated WK extracted from wool; Standard mixtures including cytochrome C (12 500 Da), aprotinin (6 500 Da), bacillus (1 450 Da), acetyl-alanine-tyrosine-arginine (451 Da) and ethine-ethyl-alanine (189 Da). The right axis shows the fitting curve of standard mixtures.

Supporting tables

Table S1. Mechanical properties of films prepared by different methods.

Film	Young's Modulus (MPa)	Elongation (%)	TS (MPa)	Hardness (N)	Toughness (mm)
RP	1.09 ± 0.18[a]	42.41 ± 1.15[c]	4.78 ± 0.29[b]	4.86 ± 0.34[a]	2.27 ± 0.02[b]
RP-MA	0.87 ± 0.04[ab]	58.82 ± 7.63[c]	4.51 ± 0.58[b]	1.79 ± 0.16[c]	1.66 ± 0.02[c]
RP-WK	0.81 ± 0.03[b]	102.79 ± 11.52[a]	9.04 ± 0.02[a]	3.39 ± 0.23[b]	2.41 ± 0.05[a]
RP-CPP	0.26 ± 0.06[c]	90.18 ± 0.15[b]	2.05 ± 0.02[c]	1.14 ± 0.12[d]	2.24 ± 0.05[b]

[a] Same superscript letter indicates no significant differences ($p < 0.05$).

Table S2. The relative secondary structure of original RP, RP-MA FFP, RP-WK FFP and RP-CPP FFP.

	Original RP	RP-MA FFP	RP-WK FPP	RP-CPP FFP
α-helix (%)	17.21	27.59	14.66	16.10
β-sheet (%)	26.45	30.78	19.87	23.43
β-turn (%)	12.23	16.08	25.19	20.06
Unorder (%)	30.61	15.82	30.91	30.77

Note

Fig. S1. First, the pH 12 film-forming solution were prepared (according to the preparation method of RP FFP in this work), hereafter, different levels (0%, 0.1%, 0.5%, 1%, w/v) of malic acid were added to the FFP, and then the FFP was again adjusted back to pH 12 by using 0.01 M NaOH. After that, the film was prepared according to the post-processing steps previously described.

The film was cut into small pieces (about 1 cm^2) and fixed on a freshly cleaved mica sheet. Images were collected on an AFM (5500AFM/SPM03040136, Agilent, United States) by tapping mode. The AFM images show that the roughness of the film is slightly reduced at a low level of malic acid addition, but when the amount is 0.5% (the malic acid: protein mass ratio is 1/6), the surface of the film became significantly smoother. Therefore, we believed that enough malic acid addition can act as a filler under the higher-order assembling level of the proteins in the film.

In **Fig. S1D**, compared with RP FFP without the addition of MA, no significant changes ($p < 0.05$) of average particle size of RP were found with MA concentration up to 0.5% (w/v). While the corresponding ξ-potential absolute value was gradually decreased ($p < 0.05$), which means that the stable of RP FFP was decreased (**Fig. S1E**). At the higher MA concentration (1%, w/v), RP tended to agglomerate on a large-scale with average particle size was as high as 6525 ± 317 nm. And the corresponding ξ-potential absolute value was significantly decreased ($p < 0.01$). These results have closely related the neutralization of MA which can decrease of net charge of RP.

But, after the readjusting the pH to 12, there was no significant difference ($p < 0.05$) of the average particle size and ξ- potential value between RP FFPs with the addition of MA or not. Therefore, the agglomeration effect of MA on RP was reversible by adjusting the pH. And it can be considered that the neutralization of MA on the distance between the fiber-fiber of RPs has been eliminated by experimental design.

The cross-linking of MA with proteins was widespread,[2] so we tried to understand the effect of the addition of MA on the degree of cross-linking. The titration method reported by Xu, Helan et al.[3] was used with a slight modification to estimate the degree of cross-linking between RP and MA. Briefly, the pH 12 film-forming solution were prepared as previously introduced (Line: 64-67), and the reaction was terminated by an ice bath immediately after thermal treatment at 90 °C for one hour. After neutralizing the reaction solution with HCl, the salt and free MA in the RP FFPs was removed using a cellulose dialysis bag (8000-14000 Da, Yuanye Biotechnology Co. Ltd, Shanghai, China). Then, accurately weigh 0.2 g lyophilized powder of FFPs, dissolved in 40 mL of water and add 25 mL of standard 0.025 M HCl. The pH of the solution was fine-tuned to 2. The sample solution was then titrated with 0.025 M NaOH and the pH was recorded once per 2 mL of NaOH.

In Fig. **S1F**, the titration process was designed in two main parts. First, the excessive H^+ from excessive HCl, H^+ of COOH in RP, and H^+ extracted from NH^{3+} in RP were consumed in turn.[3, 4] Finally, excess OH^- caused the pH of the solution to rising rapidly. As the concentration of malic acid increased, the pH of the system increased when the same of volume of NaOH consumed, indicating that more and more $–COO^-$ and $–NH_2$ of RP were

reacted with MA, resulting in less and less of "available" H^+.

These results indicated that the degree of chemical cross-linking between RP and MA was increased with MA concentration, and the addition of MA also made the RP film smoother.

Fig. S2. Oscillation-frequency test was performed on a stress-controlled rheometer (DHR-2, TA Instruments, New Castle, DE, USA) with parallel plates (40 mm diameter, 1 mm gap) in the frequency range of 1-100 Hz at 25 °C of 1% viscoelastic interval. A 1.5 mL sample was added to the rheometer plate for measurements. The samples were allowed to stand for 3 min to allow for fluid recovery structure prior to the initiation of the measurement.

According to a previous study, different pectin amounts appeared to result in different structures of the protein-pectin network.[4] The addition of pectin may cause a conformational transition of protein molecules and affect the entanglement between protein molecules, thus affecting strength of protein-pectin network. In this study, 1% pectin (based protein, w/w) was added, and the rheological tests were carried to clarify the effect of pectin on protein-pectin network at this level of addition. Fig. S2 shows the storage modulus (G'), loss modulus (G") and the complex viscosity (η*) of PR-FFP (Fig. S2A) and RP-CPP FFP (Fig. S2B) as a function of angular frequency. For RP-CPP FFP, gel point appears at low frequency oscillations, while G' and G" of RP-FFP have no intersections (gel point) within the sweep range. The viscoelastic modulus (G' and G") of RP-FFP was much higher than that of RP-CPP FFP over the range tested, which could be the evidence that the combination of protein and pectin formed a relatively weaker network, under 1% pectin addition level (w/w) in this study. For complex viscosity, both decrease with increasing frequency. The sample with

added CPP has a significantly lower composite viscosity, which means a larger exchange surface area is formed.[5]

Fig. S3. XRD patterns were recorded by XRD-7000 diddractometer (Shimadzu co.,ltd., Kyoto, Japan) with CuKa radiation, scanning angular region (2 theta) performed from 5° to 50° at 1°/min. All protein films exhibited detailed diffraction patterns. Both showed a broad peak near 20.4°. Wide and broad peaks indicate good compatibility[6] between the additive and rice protein and anisotropy of films.

Fig. S4. Approximately 3.0 mg of freeze-dried powder of RP and RP FFPs were directly weighed onto an aluminum pan. The pan was hermetically sealed prior to DSC measurement. An empty aluminum pan sealed with a lid was used as a reference. 20-100 °C scanning was carried in a nitrogen atmosphere.

There are two endothermic peaks in RP, at 51.1°C and 85.7 °C, respectively. The large ΔH (57.63 J/g) of the endothermic peak at 51.1 °C may be the result of albumin denaturation[7] and hydrogen bond cleavage.[8] Considering the possible composition of rice protein and the corresponding T_d value, the broad endothermic peak around 85.7 °C was mainly due to the denaturation of rice glutelin.[9] And this ΔH (4.53 J/g) was close to the previously reported value.[9]

Under conventional processing conditions (less than 100 °C), the additive (MA, WK, CPP) did not show significant endothermic/exothermic peaks after modification of the rice protein structure, indicating that our strategies can improve the thermal stability of rice protein.

Fig. S8. The SEC-HPLC revealed partial hydrolysis of rice protein during stirring for one

hour at pH 12. Compared to free RP without aggregation, RP-WK FFP lost shoulders and sharper peaks indicating a combination of WK and RP widely occurring.

Fig. S11. Test method referring to the Chinese national recommendation standard GB/T 9350-2003 (Plastics-Homopolymer and copolymer resins of vinyl chloride Determination of pH of aqueous extract). The results showed that the pH of the aqueous extract of all the films was almost unchanged after 1 minute, and the water extract of RP film was highly alkaline, which greatly limited its application. Our proposed waste recycling strategies were milder and more friendly to the weaker acidic skin environment of the human body.

Fig. S12. Test condition: Samples were filtered through a 220 nm filter before being injected into the HPLC system (1260 infinity II, Agilent Technologies, USA). TSKgel 2000 column (7.8 mm×300 mm, 5 μm, Tosoh, Tokyo, Japan) and the separated samples were detected using a UV detector at 220 nm. The column temperature was maintained at 30 °C; the mobile phase was acetonitrile/water/trifluoroacetic acid (45/55/0.1, v/v/v); flow rate was maintained at 0.5 mL/min; injection volume was 10 μL**.**

The molecular weight of the regenerated wool keratin is approximately 17.10 kDa, which is close to the results of Wang.[10]

Table S2. The initial slope of the stress-strain curve as the Young's modulus by programming the Exponent software that comes with the texture analyzer. It can be found that the Young's modulus of RP film is significantly larger, which may be related to the higher stretching of the protein molecules caused by the high alkali conditions, which can impart mechanical strength to the protein film under low strain conditions.

References:

1 Reddy, N., Li, Y., & Yang, Y. (2009). Alkali-catalyzed low temperature wet crosslinking of plant proteins using carboxylic acids. *Biotechnology Progress*, **25**(1), 139-146.

2 Xu, H., Shen, L., Xu, L., & Yang, Y. (2015). Low-temperature crosslinking of proteins using non-toxic citric acid in neutral aqueous medium: Mechanism and kinetic study. *Industrial Crops and Products*, **74**, 234-240.

3 Stark, G. R. (1965). Reactions of Cyanate with Functional Groups of Proteins. III. Reactions with Amino and Carboxyl Groups. *Biochemistry*, **4**(6), 1030-1036.

4 J. A. Floyd, C. Siska, R. H. Clark, B. A. Kerwin and J. M. Shaver, *Anal Biochem*, 2018, **563**, 1-8.

5 A. Saint-Eve, N. Martin, H. Guillemin, E. Sémon, E. Guichard and I. Souchon, *J Agr Food Chem*, 2006, **54**, 7794-7803.

6 L. E. Abugoch, C. Tapia, M. C. Villamán, M. Yazdani-Pedram and M. Díaz-Dosque, *Food Hydrocolloids*, 2011, **25**, 879-886.

7 Q. Zhao, H. Xiong, C. Selomulya, X. D. Chen, S. Huang, X. Ruan, Q. Zhou and W. Sun, *Food Bioprocess Tech*, 2013, **6**, 1759-1769.

8 S. Gorinstein, M. Zemser and O. Paredes-López, *J Agr Food Chem*, 1996, **44**, 100-105.

9 Z. Y. Ju, N. S. Hettiarachchy and N. Rath, *J Food Sci*, 2001, **66**, 229-232.

10 K. Wang, R. Li, J. H. Ma, Y. K. Jian and J. N. Che, *Green Chem*, 2016, **18**, 476-481.